Applied Microbiology and Biotechnology (2025) 109:146
https://doi.org/10.1007/s00253-025-13535-w

BIOENERGY AND BIOFUELS

Redox regulation of hydrogen production in *Escherichia coli* during growth on by-products of the wine industry

Lusine Baghdasaryan[1,2] · Karen Trchounian[1,2] · Gary Sawers[3] · Anna Poladyan[1,2]

Received: 13 October 2024 / Revised: 5 May 2025 / Accepted: 31 May 2025

Abstract

Lignocellulosic wine grape waste (WGW) is a cheap medium for *Escherichia coli* growth and H_2 production. The current study investigated the effect of initial redox potential (oxidation–reduction potential (ORP)) on the growth, H_2 production, ORP kinetics, and current generation of the *E. coli* BW25113 parental and a mutant strain optimized for hydrogen evolution when fermenting WGW (40 g L^{-1}) hydrolysate. Bacteria were cultivated anaerobically on pre-treated WGW hydrolysate with dilutions ranging from undiluted to fourfold dilution, at pH 7.5. Notably, a twofold diluted medium, with pH adjustment using K_2HPO_4, exhibited reduced acidification, prolonged H_2 production, and enhanced biomass formation (OD_{600}, 1.5). The addition of the redox reagent DL-dithiothreitol (DTT) was found to positively influence the H_2 production of both the *E. coli* BW25113 parental and mutant strains. H_2 production started after 24 h of growth, reaching a maximum yield of 5.10 ± 0.02 mmol/L in the wild type and 5.3 ± 0.02 mmol/L in the septuple mutant strain, persisting until the end of the stationary growth phase. The introduction of 3 mM DTT induced H_2 production from the early-exponential phase, indicating that reducing conditions enhanced H_2 production. Furthermore, we assessed the efficacy of using intact *E. coli* cells (1.5 mg cell dry weight) as anode catalyst in a bio-electrochemical fuel-cell system. Whole cells of the septuple mutant grown under reduced ORP conditions yielded the highest electrical potential, reaching up to 0.7 V. The results highlight the potential of modifying medium buffering capacity and ORP as a tool to improve biomass yield and H_2 production during growth on WGW for biotechnological biocatalyst applications.

Key points

- *Grape pomace hydrolysate (GPH)'s pH positively impacts on biomass and H_2 yield*
- *GPH with reduced ORP enhanced H_2 yield in bacterial early-exponential growth*
- *GPH with reduced ORP facilitates microbial current generation in the system*

Keywords Wine waste pre-treatment · Redox regulation · Bacterial biomass · Hydrogenase enzymes · H_2 production · *Escherichia coli*

Introduction

Molecular hydrogen (H_2) is considered an environmentally clean, efficient, and renewable source of alternative energy for the future. Obtaining and producing H_2 are of great importance, especially in the transport industry, because only water vapor is released as a result of hydrogen combustion. Considerable research is now being done to obtain bio-H_2 from various industrial wastes, which are cheap carbon sources. According to scientific and public reports, the total global H_2 demand will reach 614 million t/year by 2050 (IEA 2022; Wang et al. 2019). H_2 can also be easily converted into electricity using fuel cells (Zhao et al. 2022) and is a strong contender for a future alternative energy resource

✉ Anna Poladyan
apoladyan@ysu.am

1 Department of Biochemistry, Microbiology and Biotechnology, Faculty of Biology, Yerevan State University, 1 A. Manoogian Str, Yerevan 0025, Armenia

2 Scientific-Research Institute of Biology, Yerevan State University, 1 A. Manoogian Str, Yerevan 0025, Armenia

3 Institute of Biology/Microbiology, Martin Luther University Halle-Wittenberg, Kurt-Mothes-Str. 306120, Halle (Saale), Germany

Published online: 14 June 2025

(Ferrari et al. 2022). Various types of biomass can serve as growth substrates for bacterial H_2 production, with lignocellulosic biomass being the most common. Its global annual production is estimated to be approximately 200 Bt (Ferrari et al. 2022). One such source of lignocellulose is the residue formed during wine production, which in 2020 ranged globally between 250 and 260 million hL (François et al. 2021). Currently, one of the primary challenges facing viniculture is the efficient management of the substantial volume of by-products, particularly grape pomace, generated during wine production within a limited timeframe. Traditionally, grape pomace has been recycled back to vineyards or orchards for utilization as fertilizer, a practice adopted in many countries today. However, due to environmental concerns, European Union regulations now mandate major wine producers to transport all winery by-products to designated distillation sites for alcohol, spirits, and piquette production (Commission Delegated Regulation (EU) 2018/273 of December 11, 2017, Article 14, Products). Failure to treat these by-products promptly can result in various environmental hazards, including soil and water pollution and the potential spread of diseases (Dahiya et al. 2021).

Winemaking by-products include grape pomace (commonly referred to as marc), lees (composed of dead yeast), and tartrate sediments. Grape pomace is primarily composed of grape skins, pulp, and seeds and serves as the predominant winery by-product. Approximately 80% of the waste is grape skin, 19% grape seeds, and 1% stalks. Grape stalks are lignocellulosic, and their composition includes mainly lignin (23–47%), cellulose (25–38%), and hemicelluloses (14–35%). Wine grape waste (WGW) also contains proteins, oils, polysaccharides, and phenolic compounds (12%) (Spinei and Oroian 2021). Aside from its use as a fertilizer and for animal feed, it is frequently simply dumped in landfills as natural waste. Phenolic compounds from WGW are of great interest as antioxidants, antimicrobials, and enzyme catalysts and can be effectively extracted, which contributes to the development of the viticulture ecological (eco-)economy (Natolino and Da Porto 2020). Nevertheless, in many developing countries, most major and minor wine producers simply dump grape pomace or deposit it in ponds: this leads to a significant environmental problem due to its high organic carbon content (31–54%) (Ferjani et al. 2020). The high carbohydrate content (33 g L^{-1}) in wine waste makes it a valuable substrate for biohydrogen production by microbial dark fermentation processes. Circular economy is developed on the principle that "everything is input to something else" (Longo et al. 2023). Thus, WGW can be utilized for microbial cultivation and the production of valuable products.

H_2 production or oxidation in bacteria is associated with hydrogenases (Hyd), which can be either soluble cytoplasmic or membrane-bound enzymes. In vitro, Hyd catalyze the reversible redox reaction, $H_2 \leftrightarrow 2H^+ + 2e^-$ (Peters et al. 2015). Hyd or bacterial whole cells are also recognized as effective anodic biocatalysts in biological fuel cells (BFCs). They facilitate the splitting of H_2 into $2H^+ + 2e^-$, thereby contributing to electricity (current) generation in the electrochemical system (Ferrari et al. 2022; Obileke et al. 2021; Seferyan et al. 2024).

The well-characterized model bacterium *Escherichia coli* has numerous biotechnological applications, serving as an excellent platform for the production of recombinant proteins utilized in therapeutics and industrial processes (Castiñeiras et al. 2018). *E. coli* also produces H_2 during mixed-acid fermentation of sugars and glycerol by the formate hydrogenlyase (FHL) enzyme complex, synthesizing a total of four [NiFe]-Hyd enzymes (Trchounian et al. 2012; Pinske and Sawers 2016), which operate under different physiological conditions (Trchounian et al. 2012, 2017). In [NiFe]-Hyds, the enzyme's structure is characterized by the presence of large and small subunits, each playing a critical role in the enzyme's function. The large subunit includes the active site where the catalytic reaction takes place and has a cofactor comprising nickel (Ni) and iron (Fe) ions that are essential for the enzyme's activity in hydrogen metabolism. The small subunit, on the other hand, contains iron-sulfur ([Fe-S]) clusters, which are essential for electron transfer processes within the enzyme. These [Fe-S] clusters facilitate the movement of electrons, which is necessary for the catalytic conversion of H_2 molecules. Depending on the characteristics of the external environment (such as pH, ORP, and carbon source), Hyd enzymes respond differently, increasing interest in their functional and regulatory mechanisms.

As is known, bio-H_2 is produced during dark and photofermentations, which involve a series of redox reactions. Redox potential or oxidation–reduction potential (ORP) is a critical control parameter in fermentation processes, influencing various biochemical pathways and the overall efficiency of the process (Vassilian and Trchounian 2009; Chen-Guang et al. 2017). ORP influences the whole metabolic network, including gene expression, protein synthesis, enzyme activity, and consequently metabolite generation. Because maintaining a balance of intracellular redox potential is essential for cells, controlling redox potential either within or between cells can be an effective method for redirecting metabolic flux toward desired products. This concept has been used to produce a wide variety of fermentation products (Chen-Guang et al. 2017).

A decrease in ORP during bacterial growth strongly correlates with an increase in redox processes, which is characteristic for metabolic activity and underlies cell growth. Intracellular ORP is primarily determined by the ratio of NADH to NAD^+. A high NADH/NAD^+ ratio can lead to the accumulation of intracellular metabolites and the production of unusable by-products (Huang et al. 2017). However, the intracellular

ORP is not only dependent on the NADH/NAD^+ ratio but can also be modulated by changes in extracellular ORP.

Various chemicals with higher or lower standard redox potentials than typical metabolic components can be added to the fermentation broth to modify the environmental redox potential (Xue et al. 2023); examples include hydrogen peroxide (H_2O_2), DL-dithiothreitol (DTT), and potassium ferricyanide ($K_3[Fe(CN)_6]$). Facultative anaerobes, in contrast to strict anaerobes, grow in environments with relatively high ORP values, which depend on the amount of oxygen available. To establish initial oxidative (~ +250 mV) and reductive (~ −250 mV) ORP values, the membrane-impermeant oxidizer potassium ferricyanide and the membrane-permeant reducer DTT can be employed, with potassium ferricyanide leading to a high positive ORP value, which strongly suppresses the growth of anaerobic bacteria (Poladyan et al. 2019). Usually, potassium ferricyanide at a concentration as low as 1 mM influences growth. In contrast, DTT reduces the ORP of the medium, thereby prolonging the lag and log phases of the growth of *E. coli*, with 3 mM DTT lowering the ORP from −60 to −220 mV. Higher concentrations inhibit bacterial growth. The effect of DTT on the growth of *E. coli* may be mediated by its modulation of thiol groups in membrane proteins, leading to changes such as the generation of membrane potential ($\Delta\Psi$), potassium ion accumulation, and altered activity of membrane-associated enzymes (Kirakosyan et al. 2004).

The aim of this study, therefore, was to test the effect of modulating pH and ORP in order to optimize biomass and H_2 production/oxidation using WSW hydrolysate as a growth substrate. We use the model parental strain of *E. coli*, BW25113, and an isogenic variant (BW25113*hyaB hybC hycA fdoG ldhA frdC aceE*) as a septuple mutant strain (Maeda et al. 2007). This latter septuple mutant strain lacks the capacity for H_2 oxidation and allows channeling of carbon almost exclusively to pyruvate for conversion to acetyl-CoA and formate by the pyruvate formate-lyase enzyme (Maeda et al. 2007). We make use of redox reagents to optimize the growth of *E. coli* on WGW as a carbon substrate to improve H_2 production. Moreover, we examine the application of cells grown with WGW as an anodic catalyst in a biofuel cell. These results highlight the potential of using economically viable lignocellulosic wine grape waste as a medium for biomass and H_2 production by *E. coli* and demonstrate the significance of ORP in controlling growth and H_2 production in this system.

Materials and methods

Bacterial cultivation conditions

E. coli BW25133 strain (parental strain) and the septuple mutant strain of *E. coli* (BW25113*hyaB hybC hycA fdoG ldhA frdC aceE*) were provided by Prof. T. Wood, Department of Chemical Engineering, Penn State University, USA. *E. coli* pre-cultures (inoculum) were grown under fermentative conditions in a peptone medium (PM) with 0.2% (w/v) glucose, pH 7.5, 37 °C (Trchounian et al. 2012). The bacterial inoculum (3% v/v) was then added to the prepared growth medium. Bacterial growth was determined spectrophotometrically (Cary 60 UV–vis spectrophotometer from Agilent Technologies, USA) at a wavelength of 600 nm. Bacterial specific growth rate (μ) was monitored as described (Poladyan et al. 2019). The pH of the medium was measured using a HJ1131B pH meter (Hanna Instruments, Portugal), calibrated with 0.1 M NaOH or 0.1 N HCl solutions.

Waste pretreatment

Pre-treatment of WGW (stalks and pomace) was carried out by a combination of physical and chemical methods (Taylor et al. 2019). WGW was obtained from "Wineworks" Winery (CJSC), Yerevan, Armenia. Suspensions containing 4% (w/v) WGW and 0.4% (v/v) sulphuric acid were autoclaved at 121 °C for 20 min (Daihan Scientific, South Korea) (Poladyan et al. 2018). To remove sedimented material, the suspension was centrifuged for 15 min at 7500 × *g* (Thermo Fisher Sorvall LYNX 6000, Thermo Scientific, Germany). The solutions were then diluted two- or four-fold, and the pH was adjusted to 7.5 using 1 M potassium hydrogen phosphate (K_2HPO_4) or potassium hydroxide (KOH). The pH of the medium was determined with an accuracy of 0.01 units using HJ1131B or Hi2210 pH meters (Hanna Instruments, Portugal) and a counter-selective electrode. One millimolar $K_3[Fe(CN)_6]$ (potassium ferricyanide) or 3 mM DTT (DL-dithiothreitol) was added to the growth medium as indicated (Abrahamyan et al. 2015).

Determination of oxidation–reduction potential (ORP), H_2, and H_2-oxidizing Hyd activity

The ORP of the medium was monitored using redox electrodes: platinum (Pt) (EPB-1, Measuring Instruments Enterprise, Gomel, Belarus, or PT42BNC, Hanna Instruments, Portugal) and titanium-silicate (Ti-Si) (EO-02, measuring instruments enterprise, Gomel, Belarus) electrodes (Poladyan et al. 2019). Before measurements were taken, the readings of both electrodes were tested using 0.049 M $K_3[Fe(CN)_6]$ and 0.05 M $K_4[Fe(CN)_6] \times 3H_2O$ solutions, pH 6.86. The Pt electrode is sensitive to O_2 and H_2 levels in the medium, while the Ti-Si electrode remains unaffected by the presence of O_2 or H_2 and provides an accurate ORP measurement. The combined use of these electrodes enables the simultaneous detection of H_2 and measurement of ORP

in the growth medium. H_2 yield in the liquid was estimated as described (Piskarev et al. 2019).

The H_2 yield in the gas phase was determined using gas chromatography (7820a GC-system, Agilent Technologies, USA) equipped with a thermal conductivity detector (TCD), at a flow rate of 1 mL/min, at a temperature of 50 °C in the oven and 150 °C in the column, over a period of 4 min (Lukey et al. 2010; Poole 2016). Bacteria were grown in pre-sterilized Hungate tubes at a 1/2 liquid/gas volume ratio. The gas-phase sample (200 µL) was injected onto an Agilent Technologies CP-Molsieve 5 A column (5190–1531, Agilent, Australia), 10 µm × 0.32 µm × 30 µm (Lukey et al. 2010; Poole 2016). A high-purity H_2 standard was used to calibrate the device. Given the high purity of the H_2 gas, the Hungate tube volume was considered to be fully saturated with hydrogen. Calibration was performed by introducing different volumes of pure hydrogen (40, 60, 100, 200, and 300 µL, corresponding to 1.6, 2.4, 3.3, 4.1, 8.2, 12.3 mmol L^{--1}, respectively) through the inlet. A high degree of linearity was achieved, with an R^2 value greater than 0.99, indicating a strong linear relationship between peak area and hydrogen concentration. Since the amounts of H_2 in the samples varied significantly, the quantification of each sample was based on the calibration point of the standard that recorded the area closest to the measured area. All measurements were performed in triplicate to ensure reproducibility and reliability. Conversion from gas volume to concentration was performed using the ideal gas law formula (PV = nRT). The maximum H_2 concentration was calculated using the OpenLab system.

Assessment of H_2-oxidizing Hyd activity was done using methylene blue. To harvest bacterial biomass, the suspension underwent centrifugation, followed by a second centrifugation step for 10 min at a speed of 3000–5000 × g. The resulting bacterial biomass was suspended in 300–500 µL of 50 mM K-phosphate buffer (pH 7.5). Subsequently, 1.9 mL of 50 mM K-phosphate buffer (pH 7.5) and 3 µL of 50 mM methylene blue solution were added to the cuvette (Poladyan et al. 2019; Lenz et al. 2018; Jugder et al. 2016). One unit (U) of H_2-oxidizing activity refers to the amount of enzyme required to catalyze the oxidation of 1 µmol of H_2 per minute.

Quantification of total nitrogen using Kjeldahl's method

Total nitrogen was determined according to Pang (2021), whereby 2 g wet weight of cell sample was transferred into a suitable flask, 10 mL of concentrated sulfuric acid solution and a catalyst tablet (K_2SO_4 (3.6 g) and $CuSO_4 \cdot 5H_2O$ (0.4 g), which promote digestion; nitrogen content in tablet < 20 ppm) was added, and then, the suspension was hydrolysed in the TURBOTHERM system (Gerhardt, Germany). Decomposition was carried out through temperature step transitions over 2 h, reaching a maximum temperature of 450 °C. Then, the hydrolysate was cooled and transferred to a VAPODEST 200–450 (Gerhardt, Germany) distillation system, where a 250-mL conical flask containing 50 mL of 4% (w/v) boric acid solution and an indicator (ethanol solution of methylene red and bromocresol green) had been included. The hydrolysate was decomposed by pumping 34% (w/v) NaOH and high-temperature water vapor, as a result of which about 120 mL of distillate was collected in a flask with boric acid, which was accompanied by a change in the color of the indicator. The ammonia-containing distillate was then titrated with 0.1 M HCl until the solution changed color from bluish green to pink. The calculation of the amount of nitrogen depends on the volumes of acid used for the titration of the sample and for the control.

Determination of chemical oxygen demand (COD)

Chemical oxygen demand was determined in dry pomace and in liquid samples treated by acid hydrolysis. Twenty milliliters of digestion reagent (33.3 g of mercuric sulfate ($HgSO_4$), 167 mL of sulfuric acid 96% w/v, 58.844 g of potassium dichromate ($K_2Cr_2O_7$) in 1000 mL distilled water) and 30 mL of sulfuric acid reagent (10 g of silver sulfate ($AgSO_4$) in 1000 mL of sulfuric acid 96% w/v) were added to 0.1 g of dry or 5 mL of liquid samples. The samples were placed in the TURBOTHERM system (Gerhardt, Germany) and exposed to a fixed heating block at 150 °C for 2 h. The hydrolysate was transferred to a 500-mL Erlenmeyer flask, and three drops of ferroin indicator were added. Excess potassium dichromate was titrated with 0.5 N FAS (200 g $(NH_4)_2Fe(SO_4) \cdot 6H_2O$ and 40 mL of sulfuric acid (96% w/v) in 1000 mL distilled water) solution until the color changed from light to dark green (Raposo et al. 2008).

Colorimetric determination of total carbohydrates and measurement of volatile solids (VS) (organic matter)

A 1 mL aliquot of phenol and 5 mL of 36% (w/v) sulfuric acid were added to the 2 mL carbohydrate mixture and transferred to a water bath of 25–30 °C for 10–20 min. Two milliliters of distilled water, 1 mL of phenol, and 5 mL of concentrated sulfuric acid were added to a control sample (carbohydrate-free). Absorbance of the solution was measured at a wavelength of 485 nm (Oliveira et al. 2015). For the calibration curve, a 1 mg/mL glucose solution was prepared, and then, appropriate dilutions were prepared down to 100 µg/mL. Samples were taken at different times during bacterial growth and centrifuged at 5000 rpm to remove biomass prior to measurement.

The quantitative determination of volatile solids (VS) was performed using a muffle furnace (DAIHAN Digital Muffle Furnace, Taiwan) (Zhang et al. 2019; Sołowski et al. 2020). The sample was weighed and placed in a dryer at 105 °C for 24 h. Then, the samples were placed in a muffle furnace at 550 °C for 4 h. The final mass of the sample corresponds to the content of organic carbon in the examined sample.

Electrochemical measurements

Electrochemical measurements were conducted using a double-electrode electrochemical system, outfitted with a H_2 fuel cell voltammeter (HFCV). The reference electrode was fabricated using silver ink technology (Ferrari et al. 2022; Seferyan et al. 2024). Cell suspension (3 µL) of the parental strain was immobilized onto the testing micro-strip using a 3 mM KCl solution and a 0.8% (w/v) bacteriological agar support. Biological samples were immobilized between two thin-layer electrodes. After immobilization, H_2 was introduced into the system, and the ensuing current was monitored using LabVIEW software (Seferyan et al. 2024).

Processing of data

Data were obtained from five different experiments. The data were processed using Microsoft Excel 2016. Student's *t*-test (*P*) was chosen to indicate the error range for each experiment. A difference was considered significant when $P < 0.05$.

Results

Pre-treatment of WGW and cultivation and H_2 production of *E. coli* BW25113 (parental strain): effect of pH

The 4% (w/v) WGW suspension was physicochemically treated as previously described (Poladyan et al. 2018, 2020). The VS, carbohydrate, and nitrogen amounts were estimated to be ~ 28 g L^{-1}, 20 g L^{-1}, and 2.8 g L^{-1}, respectively, in the pre-treated WGW. As a typical waste indicator, the COD of the WGW hydrolyzate was determined to be 32 g L^{-1}. The formation of *E. coli* BW25113 biomass and the decline of ORP, followed by acidification of the environment, were observed (Fig. 1).

When the pH was adjusted with KOH, a pronounced acidification of the growing culture from 7.5 to 4.6 occurred after 24 h of growth (Fig. 1A). Whereas in the case of pH adjustment with K_2HPO_4 buffer, the maximum decrease in pH from the initial value was observed after 24 h of growth and was recorded as pH 6.6; after 48 h, the medium became basic again (Fig. 1A).

Maximum growth (OD_{600}, ~ 1.5) of *E. coli* BW25113 (parental strain) was observed after 48 h in twice-diluted WGW with an initial content of ~ 10 g L^{-1} total carbohydrate and 1.4 g L^{-1} nitrogen and when the pH of the medium was adjusted with K_2HPO_4. However, a prolonged (~ 5 h) lag phase in growth was observed, and the culture continued to gain biomass up to 72 h (Fig. 1B) with a specific growth rate (µ) of ~ 0.48 ± 0.02 day^{-1}.

Total nitrogen and carbohydrate consumption were monitored during 168 h of bacterial cultivation (Fig. 2). After 24 h, total nitrogen decreased by approximately 2.6-fold, reaching negligible amounts after 72 h of cultivation (Fig. 2A). A sharp reduction in carbohydrate levels was also observed after 24 h of bacterial growth and continued to decrease more slowly up to 168 h of cultivation (Fig. 2B).

H_2 production was estimated both in the liquid and gas phases. Monitoring H_2 production yields in the liquid phase allows us to follow production from the early stages. During bacterial growth up to 24 h, a decrease of the Pt electrode reading from a positive value (+ 100 mV ± 10 mV) to a low, negative value of − 400 ± 10 mV was observed (Fig. 3A). After 24 h and for the non-diluted and two- and four-fold diluted WGW hydrolysate samples (initial ~ 10 g L^{-1} total carbohydrate and 1.4 g L^{-1} nitrogen and ~ 5 g L^{-1} total carbohydrate and 0.7 g L^{-1} nitrogen, respectively), the values of ORP decreased from a positive to a negative value, down to as low as − 530 mV, which correlated with the production of H_2 under WGW fermentation conditions. H_2 production was maintained in all samples even after 48 h of growth. H_2 yield in the liquid and gas phases was determined in two- and four-fold diluted WGW media when the pH was adjusted with K_2HPO_4 or KOH.

Compared to the undiluted WGW sample, the H_2 yield was shown to be approximately threefold higher in medium containing the two-fold diluted WGW hydrolysate and when the pH of the medium was adjusted with K_2HPO_4. H_2 production continued after 48 h in all samples. Meanwhile, H_2 production in *E. coli* BW25113 was observed only after 24 h in two- and four-fold diluted WGW medium when the pH was adjusted with KOH, and no H_2 production was observed either after 24 h or 48 h of growth in the undiluted sample.

As anticipated, these results show that the maximum growth (biomass production) and prolonged H_2 production of *E. coli* BW25113 bacteria in the WGW medium were maintained in the medium with high buffering capacity. Based on this data, further experiments were conducted using a medium with two-fold diluted WGW hydrolysate (initial 10 g L^{-1} total carbohydrate and 1.4 g L^{-1} nitrogen) with the pH adjusted using K_2HPO_4. The H_2 production yield in the liquid phase of the parental strain after 24 h of growth was approximately 5.1 mmol L^{-1} (Table 1), whereas a comparable yield in the gas phase was only achieved after 72 h of growth (Fig. 3B).

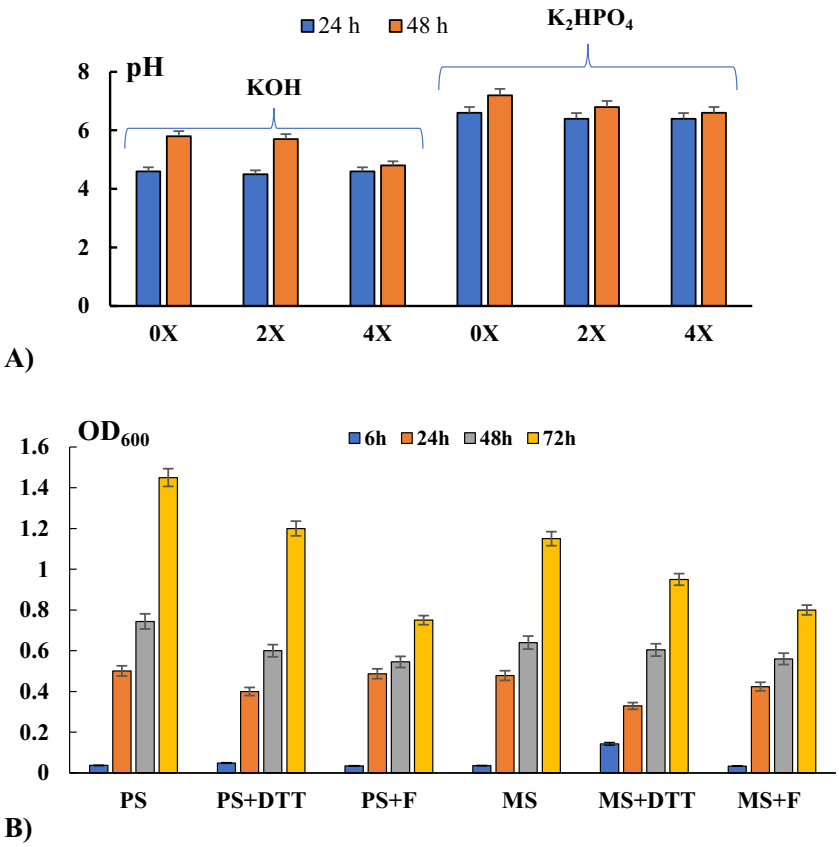

Fig. 1 Change in pH during 48 h cultivation of *E. coli* BW25113 (**A**) and biomass formation (OD_{600}) (**B**) using WGW hydrolysate ($n = 5$, $p < 0.05$). The pH of the medium was adjusted either by 1 M KOH or by K_2HPO_4. Bacteria were grown anaerobically at an initial pH of 7.5 and at 37 °C. In figure **B**, biomass formation was monitored in 2X diluted WGW. OX, 2X, and 4X refer to undiluted, twofold diluted, and fourfold diluted hydrolysates, respectively. DTT—DL-dithiothreitol, F—potassium ferricyanide, PS—parental strain, MS—the septuple mutant

Effects of redox reagents

Determination of ORP (redox potential) values signifies the ability of microorganisms to adapt their metabolic capacity to environmental redox changes (Vassilian and Trchounian 2009; Chen-Guang et al. 2017). The extracellular redox potential differs from the intracellular redox state due to the separation provided by the plasma membrane and the maintenance of cellular redox homeostasis. Environmental factors play a crucial role in indirectly altering the cellular redox potential. According to the Nernst equation, redox potential is determined as the ratio of the oxidative state to the reductive state at a constant temperature, which remains a fixed parameter in most biological processes (Vassilian and Trchounian 2009).

In this study, the redox regulation of biomass and H_2 production during WGW fermentation of *E. coli* strains was investigated. Redox reagents, such as the impermeable oxidizer potassium ferricyanide ($K_3[Fe(CN)_6]$; K-ferricyanide) and the membrane-permeant reducer DL-dithiothreitol (DTT), were used. Supplementation with 3 mM DTT reduced the initial ORP to − 250 mV, whereas 1 mM K-ferricyanide maintained a positive ORP of + 250 mV (Fig. 3A). The effects of these reagents on the growth parameters and redox kinetics of the *E. coli* parental strain and the septuple mutant strain (BW25113*hyaB hybC hycA fdoG ldhA frdC aceE*) were investigated. In the mutant strain, glucose metabolism is directed mainly to formate formation via deleting various genes responsible for H_2 oxidation (*hyaB* encoding the large subunit of Hyd-1 and *hybC* the large subunit of Hyd-2), periplasmic formate oxidation, inactivating lactate dehydrogenase, fumarate reductase, and pyruvate dehydrogenase (Wood et al. 2007).

H_2 production was stimulated in the DTT-supplemented samples (Table 1, Fig. 3B). The Pt electrode reading decreased within the first hour of growth to − 470 ± 10 mV, and H_2 production was observed accordingly, which continued until 72 h of cultivation for the parental strain. In the multiple knock-out mutant, the decrease in the ORP reading was also observed already after 3 h (− 430 ± 10 mV) (Fig. 3A, Table 1). Without DTT, H_2 production was only recorded starting from 24 h of cultivation (Fig. 3A).

During cultivation of the parental strain and in the presence of DTT, H_2 production attained a maximum yield of 5.1 mmol L^{-1} (Table 1). The inhibitory effect of K-ferricyanide on the parental strain was evident, and H_2 production was observed only after 24 h of cultivation and showed a lower yield compared to the other samples (Fig. 3B, Table 1). Meanwhile, no particularly strong effect of K-ferricyanide was observed in the mutant strain compared to the control (K-ferricyanide-free medium). The maximum H_2 yield was recorded at 24 h of cultivation in the control and K-ferricyanide-treated samples, with values of 5.25 mmol L^{-1} and 5.0

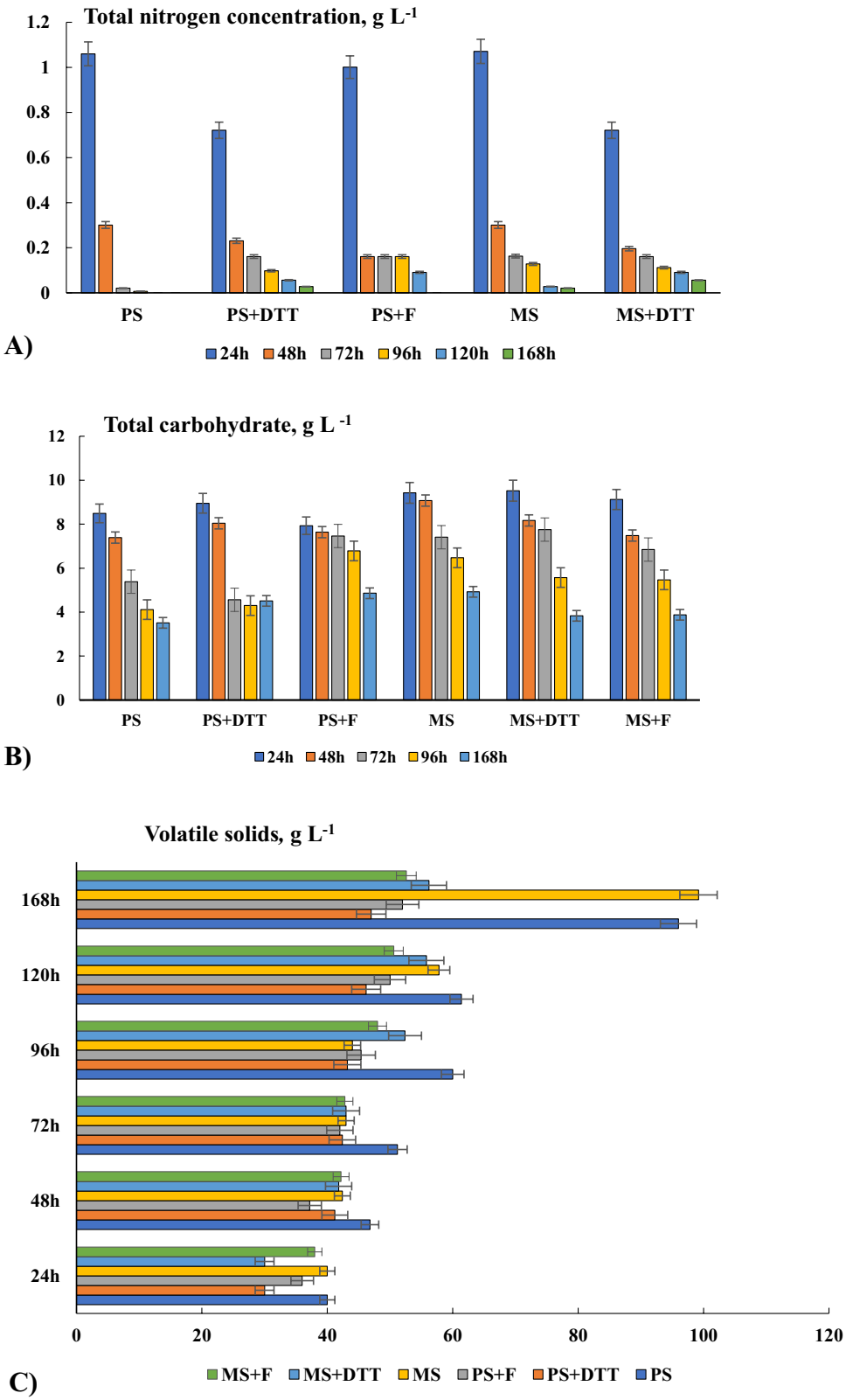

Fig. 2 Total nitrogen concentration (**A**), total carbohydrate (**B**), and volatile solids (VS) content (**C**) of *E. coli* BW25113 parental strain (PS) and the septuple mutant (MS) in the presence of redox reagents during growth in 2X diluted WGW at pH 7.5 are shown. Bacteria were grown anaerobically. An average of 3 independent experiments is presented, $p < 0.05$. DTT—DL-dithiothreitol, *F*—potassium ferricyanide

mmol L^{-1}, respectively (Table 1). Furthermore, H_2 production continued until the final stage of cultivation (Fig. 3B). In the sample containing DTT and K-ferricyanide, bacterial biomass formation and μ (per day) were reduced ~ 1.2 and 1.7-fold, respectively (Fig. 1B). Similar effects were shown for the mutant strain cultivated under the same condition.

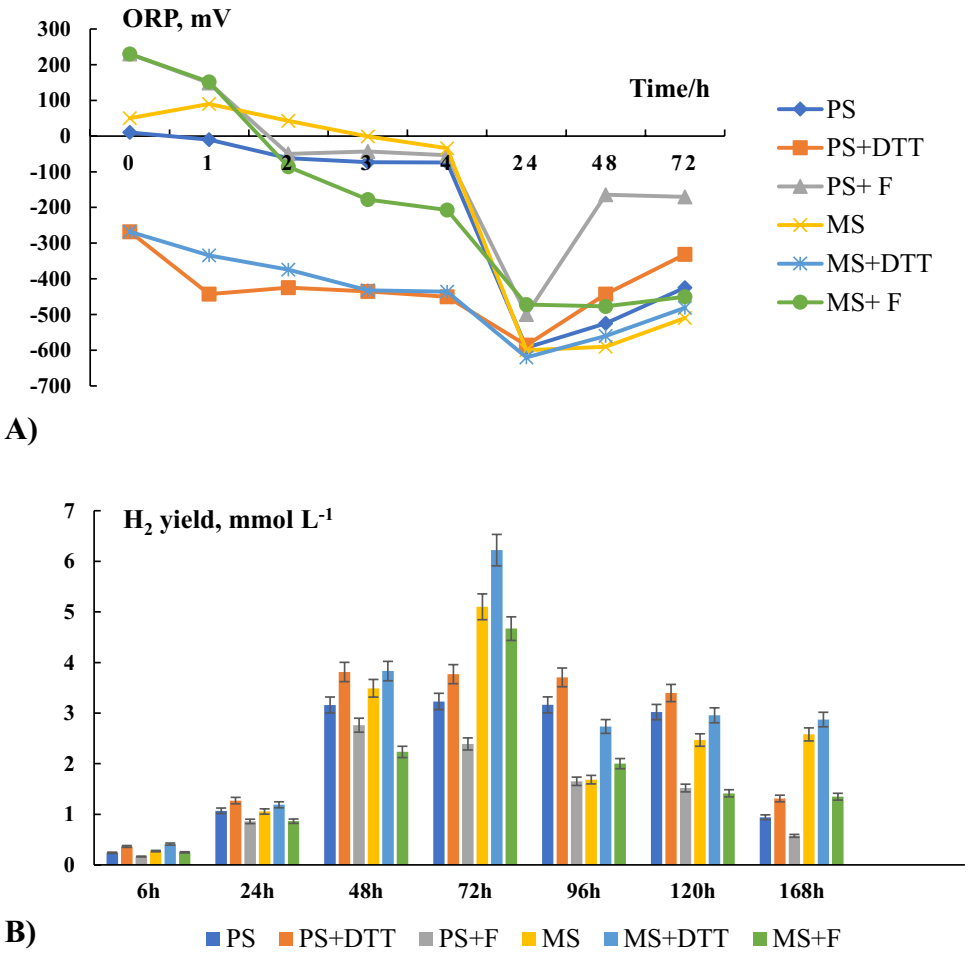

Fig. 3 Changes in ORP (**A**) and H_2 production yield in the gas phase (**B**) of *E. coli* BW25113 and mutant strain in the presence of redox reagents during growth in 2X diluted WGW at pH 7.5. Bacteria were grown anaerobically. ORP was measured with a platinum electrode (Pt) and expressed in mV (Ag/AgCl (saturated with KCl)). An average of 3 independent experiments is presented, $p < 0.05$. DTT—DL-dithiothreitol, F—potassium ferricyanide, PS—parental strain, MS—septuple mutant

Table 1 H_2 yield in *E. coli* parental strain (PS) and mutant strain (MS) during growth in two-fold diluted WGW growth medium

Samples	H_2 production yield, liquid phase, mmol L^{-1}				
	1 h	**2 h**	**24 h**	**48 h**	**72 h**
PS	–	–	5.10	1.5	–
PS + DTT	1.50	1.40	5.10	1.52	0.80
PS + F	–	–	1.6	–	–
MS	–	0.80	5. 25	3.68	1.50
MS + DTT	0.75	0.80	5.24	1.36	0.85
MS + F	–	–	5.00	2.25	1.40

H_2 yield is presented with an accuracy of ± 0.02 mmol/L

DTT DL-dithiothreitol, *F* potassium ferricyanide

In the case of control experiments (redox reagent-free medium), the maximum assimilation of carbohydrates was observed after 24 h of cultivation and measured at ~ 73 to 78% of the levels compared to media containing DTT and K-ferricyanide. Generally, the parental strain showed a 25% reduction in the uptake of carbohydrate compared with when redox mediators were added to the growth medium (Fig. 2A). Interestingly, K-ferricyanide-containing samples of both strains showed a more active utilization of carbohydrates up to 48 h of cultivation compared to the other growth media, after which the rate of carbohydrate consumption slowed in the parental strain, while it remained steady for the septuple mutant.

The initial nitrogen concentration of 1.4 g L^{-1} in the medium decreased gradually as the bacteria grew, eventually approaching complete depletion (Fig. 2B). At the 48-h timepoint of cultivation, between 78 and 93% of the total nitrogen had already been assimilated (Fig. 2B). Maximal nitrogen uptake was observed in DTT- and in K-ferricyanide-containing cells of the parental strain, while for the mutant maximal uptake, it occurred by 48 h of cultivation (Fig. 2B).

During bacterial growth, quantitative changes in volatile solids (VS) using a muffle furnace were observed. Production of VS is frequently used in waste valorization and anaerobic digestion studies to evaluate the biodegradability and transformation of organic content in complex feedstocks (Zhang et al., 2018). The amount of VS in the hydrolyzate of WGW was found to be 14 g L^{-1} (Fig. 2C).

Along with bacterial growth, VS also increased, reaching a maximum of 96 ± 0.02 g L^{-1} and 99.2 ± 0.02 g L^{-1} by the end of cultivation for the parental and mutant strains, respectively. Notably, during the cultivation of the parental strain using DTT-containing medium, the VS consistently remained lower than in the K-ferricyanide-containing medium throughout the period of cultivation, while in the case of the mutant strain, the K-ferricyanide-containing sample had a lower VS than the DTT-containing sample (Fig. 2C). It is noteworthy that the change in the amount of carbon accumulation correlated with H_2 production, particularly around the 72 h of cultivation (Fig. 2C). The mutant strain showed slightly more H_2 production and less organic carbon formation, indicating that assimilated carbon was directed toward formate generation, which is the electron source for H_2 production (Maeda et al 2018), rather than biomass. H_2 production was measured in the gas phase of all samples from 6 h onwards (Fig. 3B).

Compared to the parental strain, an intensive H_2 production was observed in the septuple mutant in both liquid and gaseous phases; DTT had a stimulating effect on H_2 production in both strains at the beginning of the exponential phase of growth (Table 1, Fig. 3B) with DTT stimulating the production of H_2 ~ 1.2- to 1.3-fold. The maximum yield of H_2 in the presence of DTT was observed at 72 h, reaching 6 mmol L^{-1} (Fig. 3B), while in both samples containing ferricyanide, H_2 production was inhibited until the latter stage of cultivation. Beginning around 72 h, the amount of H_2 began to decrease, presumably partially due to bacterial H_2 oxidation by the parental strain.

H_2 production yield and rate in the gas phase by *E. coli* parental and mutant strains during anaerobic digestion of WGW per OD and total carbohydrates (TCs) utilized at 72 h of growth were evaluated, and the data are presented in Table 2. For the parental strain, H_2 production yield and rate per total carbohydrates were ~ 1.7 mmol L^{-1} and 0.6 mmol day^{-1}, respectively. These results show that in comparison to control (parental strain), the yield and rate of H_2 production per OD and TCs in the gas phase for the septuple mutant with DTT supplementation were stimulated ~ two– to three-fold.

Electrochemical activities of *E. coli* cells grown on WGW

The activity of Hyd enzymes in H_2 oxidation was tested in cells during growth in WGW medium and in the presence of redox reagents under pH 7.5 conditions. All samples exhibited rapid decolorization of methylene blue, indicating the H_2-oxidizing capability of Hyd enzymes. In the parental strain, after growth in media containing DTT and K-ferricyanide, approximately 2 and 1.2 times greater H_2-oxidizing Hyd activity was observed, respectively. Subsequently, we tested the electrochemical activities of *E. coli* cells cultivated in WGW-containing media as an anode catalyst (Fig. 4). A total of 1.5 mg CDW of bacterial whole cells were immobilized on the micro-strips (sensors) using 0.8% (w/v) agar with the addition of 3 mM KCl (Seferyan et al. 2024). Current generation was detected in all samples (Fig. 4) as long as H_2 was supplied. Cells of the parental strain cultivated in the redox reagent–free medium had a potential of ~ 0.45 ± 0.05 V, while the mutant showed a ~ 1.6-fold increase in voltage, attaining a value of 0.63 ± 0.05 V and 0.69 ± 0.03 V after cultivation in a DTT-containing medium. However, current generation was low in the cells grown in the presence of K-ferricyanide (Fig. 4).

Discussion

WGW is rich in carbohydrates, making it a promising and economically viable resource for obtaining bio-H_2 through bacterial fermentation. According to the literature, there are various methods to use WGW as an energy source, particularly for H_2 production (Zavala-Méndez et al. 2022; Garrido et al. 2024; Spinei and Oroian 2021). Among these methods are the gasification models, which demonstrate the feasibility of converting biomass into syngas, which

Table 2 H_2 production yield and rate in the gas phase by *E. coli* parental strain (PS) and mutant strain (MS) during anaerobic digestion of two-fold diluted WGW per OD and total carbohydrates (TCs) utilized, at pH 7.5 and 72 h of growth

E. coli strains	H_2 production yield mmol $L^{-1}OD^{-1}$	H_2 production yield mmol L^{-1} g^{-1} TCs	H_2 production rate mmol L^{-1} day^{-1} g^{-1} TCs
PS	2.3	1.7	0.6
PS + DTT	3.1	1.5	0.5
PS + F	1.5	1.3	0.3
MS	4.4	3.8	1.3
MS + DTT	6.6	5.1	1.7
MS + F	3.9	3.4	1.0

H_2 yield and rate are presented with an accuracy of ± 0.02 mmol/L

DTT DL-dithiothreitol, *F* potassium ferricyanide

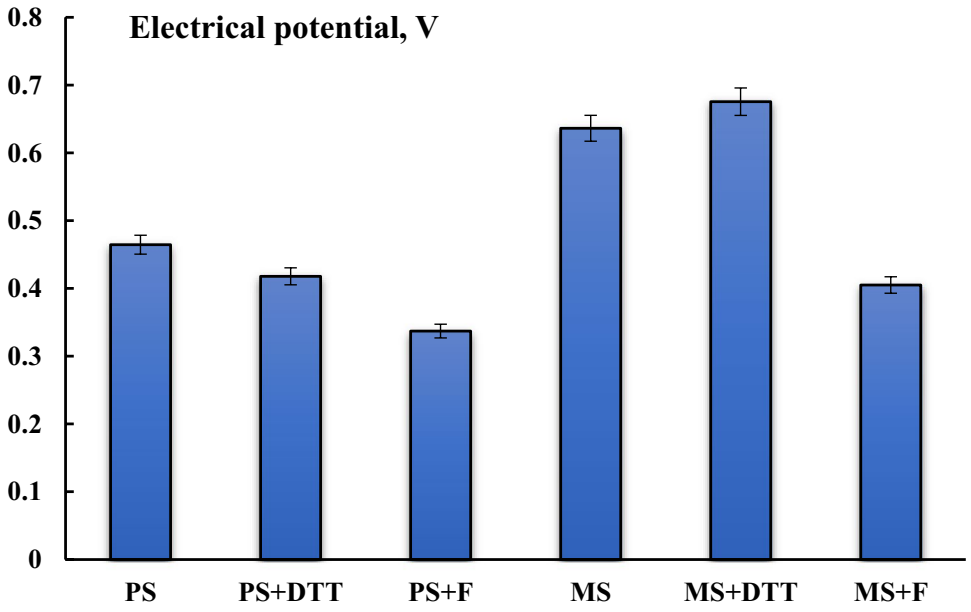

Fig. 4 Electrical potential formation with bacteria grown in WGW medium: PS—parental strain, MS—mutant strain, DTT—dithiothreitol, F—potassium ferricyanide. Bacterial whole cells (1.5 mg CDW) were immobilized on micro-strips with a volume of 3 µL, $n = 5$, $p < 0.05$. The system operated at 37 °C

can then be used for H_2 production. This process involves the high-temperature conversion of organic materials into a gas mixture primarily composed of H_2 and CO. One hectare of harvested grapes can significantly contribute to H_2 formation, with annual estimates reaching 156.6 t (Garrido et al. 2024). An interaction between lactic acid bacteria and H_2-producing bacteria was demonstrated, resulting in a H_2 yield of 1.1 ±0.4 mmol L^{-1} H_2. This microbial syntrophic association underscores the importance of understanding microbial community structure in optimizing H_2 production from grape pomace (Zavala-Méndez et al. 2022). Studies also indicate that the natural microbial communities present in WGW are as effective in producing H_2 as heat-treated exogenous inoculant. The dark fermentation process using WGW has achieved 1.6 mol of H_2 per mole of hexose. In the context of endogenous fermentation, approximately 65% of species were affiliated with the family *Clostridiaceae* (François et al. 2021).

In our study, we investigated the use of WGW as a nutrient source for *E. coli* cultivation. Lignocellulosic WGW underwent physicochemical treatment, which enabled the extraction of monosaccharides, organic and amino acids, minerals, and other components (Poladyan et al. 2018; Kumar and Sharma 2017). Carbon and nitrogen are essential nutrients for microbial growth, with carbon serving as an energy source and nitrogen necessary for protein and nucleic acid synthesis (Chen and Strevett 2003; Heeswijk et al. 2013; Heeswijk et al. 2023). When nitrogen is the limiting factor, *E. coli* exhibits a lower specific growth rate and growth yield, increased lipopolysaccharide production efficiency, and a more hydrophilic surface compared to cultures grown without carbon and nitrogen limitations (Chen and Strevett 2003). The required macronutrients for anaerobic digestion (AD) are often assessed using the carbon to nitrogen (C/N) ratio. A high C/N ratio during AD digestion can slow down biodegradation due to nitrogen deficiency and excess volatile fatty acid production. Conversely, a low C/N ratio can result in excessive ammonia, causing unpleasant odors and inhibition of anaerobic microbes. In this current study, the total amounts of nitrogen, carbohydrates, and carbon were estimated in the WGW hydrolysate. Bacterial growth was observed in WGW hydrolysate with a C/N ratio of 10, and the consumption of nitrogen and carbohydrates monitored was in accordance with *E. coli* growth. The assimilated material was directly proportional to bacterial growth and H_2 production. An increase in VS was observed following bacterial growth.

The pH of WGW hydrolysate was adjusted to 7.5 using KOH and K_2HPO_4. As is characteristic of dark fermentation, the utilization of WGW hydrolysate by the *E. coli* parental strain led to acidification of the medium due to accumulated fermentation products. More acidification was observed in the medium using KOH to adjust the pH, which negatively affected both bacterial growth and H_2 production. Strongly acidic conditions inhibit the activity of Hyd and consequently H_2 production (Liu and Li 2013; Maeda et al. 2018). Therefore, compared to KOH, the adjustment of the growth medium with K_2HPO_4, which has a considerably higher buffering capacity, resulted in improved biomass and H_2 production.

The impact of initial ORP on bacterial biomass formation, H_2 production, and current generation in the electrochemical system was investigated and revealed that H_2 production can be controlled by supplying oxidants and reductants. The membrane impermeant oxidizing agent ferricyanide induced a positive ORP and suppresses growth of

E. coli and decreases acidification of the medium. On the other hand, increasing reducing conditions with DTT led to increased formation of formic acid by *E. coli* (Poladyan et al. 2019). ORP is also crucial in regulating Hyd activity and H_2 production or its oxidation in bacteria. Hyd enzymes are sensitive to the redox state of their environment, and optimal ORP conditions can enhance their activity, boosting Hyd production (Vassilian and Trchounian 2009; Poladyan et al. 2012; Abrahamyan et al. 2015). Conversely, suboptimal ORP levels can inhibit Hyd activity, thereby reducing H_2 yield (Kirakosyan et al. 2004). Maintaining an appropriate ORP can help sustain the activity of the Hyd enzymes, thus supporting continuous Hyd production. In electrochemical systems, adjusting the ORP can also influence the electron flow and energy balance, further affecting hydrogen production and the utility of the cells for current generation.

The results presented in this study show that setting optimal reducing conditions using DTT stimulates H_2 production yield and rate during the early log growth phase. The results align with data obtained from peptone medium with glucose-fermented cells, where hydrogen production was enhanced in *E. coli* Hyd-1- and Hyd-2-negative mutants at pH 7.5 (Abrahamyan et al. 2015; Maeda et al. 2018; Poladyan et al. 2018). Additionally, DTT stimulation increased H_2 production at both pH 5.5 and 7.5 (Abrahamyan et al. 2015). Hyd-1 and Hyd-2 are primarily recognized as H_2-oxidizing enzymes. Their genetic inactivation has been shown to stimulate H_2 production in *E. coli* (Poladyan et al. 2018). In the mutant strain used in the current study, the observed increased H_2 production is likely linked to the lack of Hyd-1 and Hyd-2 (Trchounian et al. 2012; Abrahamyan et al. 2015). Additionally, the other mutations introduced into the modified strain stimulate formic acid production, which is the inducer of H_2 production by the formate hydrogenlyase system (Rossmann et al. 1991; Maeda et al. 2007). DTT supplementation likely facilitates this process, thereby enhancing H_2 production. K-ferricyanide slows the process of acidification, allowing the mutant cell to produce H_2 for a longer period. However, this delay also means that H_2 production begins somewhat later, as it takes time for the ORP to decrease to the optimal level for Hyd-3 synthesis. The mutant strain carries multiple deletions, including in particular the *ΔhyaB* and *ΔhybC* mutations that disrupt the ability of the strain to oxidize any H_2 produced, resulting in better H_2 production. Moreover, the *ΔhycA* mutation prevents a negative regulator of H_2 production from being made. As a result, the overall capacity for H_2 production by the mutant strain remained unaffected by the oxidant (K-ferricyanide). This reduced sensitivity suggests a fundamental shift in the strain's metabolic response and redox regulation compared to the wild type.

Microbial FC has been investigated to generate electricity by electrochemically active bacteria for a more than a decade (Zhang et al. 2017; Ferrari et al. 2022). Cells grown on WGW exhibit electrochemical activity as anodic catalysts in the system. K-ferricyanide-grown cells show poorer electrochemical activity. Compared to the parental strain, the mutant showed higher electrical activity, and DTT only slightly enhanced this electricity generation. The lack of Hyd-1 and Hyd-2 likely was responsible for the improved electrical capacity of the mutant cells, although the effects of the other mutations cannot be ruled out. In particular, Hyd-3 and possibly Hyd-4 are presumably key to supporting the current generation. Although it has been shown that Hyd-3 and Hyd-4 operate toward H_2 production, they are reversible under certain conditions (Maeda et al. 2007; Abrahamyan et al. 2015) and possibly also function in the Hyd-oxidizing mode within the electrochemical system. It was demonstrated that FHL can operate in two different modes depending on the environmental conditions; for example, when CO_2 and H_2 are pressurized, FHL functions as a hydrogen-dependent CO_2 reductase (Roger et al. 2018). There might be a possibility for FHL-dependent hydrogen-oxidation, but this requires considerably more experimentation. Future studies are needed to elucidate the electron transfer mechanism in this system.

Author Contribution AP conceived and designed the study. AP and KT wrote the manuscript. LB performed the experiments and analysed the data. GS edited the manuscript and gave recommendations for the experiment. All authors read and approved the manuscript.

Funding This work was supported by the grant [21 AG-1 F043] from the State Committee of Science, Ministry of Education, Science, Culture, and Sport of Armenia to LB, GS, AP.

Data availability The authors declare that the data supporting the findings of this study are available within the paper. Should any raw data files be needed in another format, they are available from the corresponding author upon reasonable request.

Declarations

Ethics approval and consent to participate This article does not contain any studies with animals or human participants performed by any of the authors.

Conflict of interest The authors declare no competing interests.

References

Abrahamyan V, Poladyan A, Vassilian A, Trchounian A (2015) Hydrogen production by *Escherichia coli* during glucose fermentation: effects of oxidative and reductive routes used by the strain lacking hydrogen oxidizing hydrogenases 1 (hya) and 2 (hyb). Int J of Hyd Energy 40(24):7459–7464. https://doi.org/10.1016/j.ijhydene.2015.02.006

Castiñeiras TS, Williams SG, Hitchcock AG, Smith DC (2018) *E. coli* strain engineering for the production of advanced biopharmaceutical products. FEMS Microbiol Lett 365(5):162. https://doi.org/10.1093/femsle/fny162

Chen G, Strevett KA (2003) Impact of carbon and nitrogen conditions on *E. coli* surface thermodynamics, Colloids and Surf B. Biointerfaces 28:2–3,135–146. https://doi.org/10.1016/S0927-7765(02)00143-1

Chen-Guang L, Jin-Cheng Q, Yen-Han L (2017) Fermentation and redox potential. Edited by Angela Faustino Jozala Chapter 2:22. https://doi.org/10.5772/64640

Dahiya S, Chatterjee S, Sarkar O, Mohan SV (2021) Renewable hydrogen production by dark-fermentation: current status, challenges and perspectives. Bioresour Tech 321:655. https://doi.org/10.1016/j.biortech.2020.124354

Ferjani AI, Jellali S, Akrout H, Limousy L, Hamdi H, Thevenin N, Jeguirim M (2020) Nutrient retention and release from raw exhausted grape marc biochars and an amended agricultural soil: static and dynamic investigation. Envr Techn Innov 19:2352–1864. https://doi.org/10.1016/j.eti.2020.100885

Ferrari IV, Pasquini L, Narducci R, Sgreccia E, Di Vona ML, Knauth PA (2022) Short overview of biological fuel cells. Membranes J 12:427. https://doi.org/10.3390/membranes12040427

François E, Dumas C, Gougeon RD, Alexandre H, Vuilleumier S, Ernst B (2021) Unexpected high production of biohydrogen from the endogenous fermentation of grape must deposits. Bioresour Tech p 320, Part A. https://doi.org/10.1016/j.biortech.2020.124334

Garrido RA, Manrique R, Fredes J, Rodriguez P, Rodríguez A, Serafini D, Mena M, Masip Y, Díaz I (2024) Evaluating hydrogen production from grape pomace gasification: unveiling the potential for Chile's wine industry and its solid waste recovery as energy source. J Renew Energy 223:119953. https://doi.org/10.1016/j.renene.2024.119953

Heeswijk WC, Westerhoff HV, Boogerd FC (2013) Nitrogen assimilation in *Escherichia coli*: putting molecular data into a systems perspective. Microbiol Mol Biol Rev 77(4):628–695. https://doi.org/10.1128/MMBR.00025-13

Huang T, Tan H, Lu F, Chen G, Wu Z (2017) Changing oxidoreduction potential to improve water-soluble yellow pigment production with *Monascus ruber* CGMCC 10910. Microb Cell Fact 16:208. https://doi.org/10.1186/s12934-017-0828-0

IEA (2022) Global hydrogen review, IEA. Paris, Licence: CC BY 4.0. https://www.iea.org/reports/global-hydrogen-review-2022

Jugder BE, Lebhar H, Aguey-Zinsou KF, Marquis CP (2016) Production and purification of a soluble hydrogenase from *Ralstonia eutropha* H16 for potential hydrogen fuel cell applications. MethodsX 3:242–250. https://doi.org/10.1016/j.mex.2016.03.005

Kirakosyan G, Bagramyan K, Trchounian A (2004) Redox sensing by *Escherichia coli*: effects of dithiothreitol, a redox reagent reducing disulphides, on bacterial growth. Biochem Biophys Res Commun 325:803–806. https://doi.org/10.1016/j.bbrc.2004.10.119

Kumar AK, Sharma S (2017) Recent updates on different methods of pretreatment of lignocellulosic feedstocks: a review. Bioresour Bioprocess 4:7. https://doi.org/10.1186/s40643-017-0137-9

Lenz O, Lauterbach L, Frielingsdorf S (2018) O_2-tolerant [NiFe]-hydrogenases of *Ralstonia eutropha* H16: physiology, molecular biology, purification, and biochemical analysis. Methods Enzymol, Chapter Five 613:117–151. https://doi.org/10.1016/bs.mie.2018.10.008

Liu H, Li Y (2013) Hydrogen production from organic wastes by anaerobic fermentation: a review. Renew and Sustain Energy Rev 25:671–682. https://doi.org/10.1016/B978-0-444-59555-3.00006-4

Longo S, Cellura M, Le Quyen L, Nguyen TQ, Rincione R, Guarino F (2023) Circular economy and life cycle thinking applied to the biomass supply chain: a review. J Renew Energy 220:119598. https://doi.org/10.1016/j.renene.2023.119598

Lukey MJ, Parkin A, Roessler MM, Murphy BJ, Harmer J, Palmer T, Sargent F, Armstrong AF (2010) How *Escherichia coli* is equipped to oxidize hydrogen under different redox conditions. J Biol Chem 285:3928–3938. https://doi.org/10.1074/jbc.M109.067751

Maeda T, Sanchez-Torres V, Wood T (2007) Enhanced hydrogen production from glucose by metabolically engineered *Escherichia coli*. Appl Microbiol Biotechnol 77:879–890. https://doi.org/10.1007/s00253-007-1217-0

Maeda T, Tran KT, Yamasaki R, Wood KT (2018) Current state and perspectives in hydrogen production by *Escherichia coli*: roles of hydrogenases in glucose or glycerol metabolism. Appl Microbiol Biotechnol 102:2041–2050. https://doi.org/10.1007/s00253-018-8752-8

Natolino A, Da Porto C (2020) Kinetic models for conventional and ultrasound assistant extraction of polyphenols from defatted fresh and distilled grape marc and its main components skins and seeds. Chem Eng Res des 156:1–12. https://doi.org/10.1016/j.cherd.2020.01.009

Obileke K, Onyeaka H, Meyer EL, Nwokolo N (2021) Microbial fuel cells, a renewable energy technology for bio-electricity generation. Electrochem Commun 125:107003. https://doi.org/10.1016/j.elecom.2021.107003

Oliveira L, Costa M, de Sousa HA, Blum J, Silva G, Abreu M, Maia D (2018) Characterization of organic wastes and effects of their application on the soil. J Agric Sci 10:291. https://doi.org/10.5539/jas.v10n6p291

Pang YL (2021) Protein determination by Kjeldahl method. In: Hasegawa H (ed) AquaDocs. E-Publishing Inc, Singapore, p B-1.1-B-1. http://aquaticcommons.org/id/eprint/26807

Peters JW, Schut GJ, Boyd ES, Mulder DW, Shepard EM, Broderick JB, King PW, Adams MW (2015) [FeFe]-and [NiFe]-hydrogenase diversity, mechanism, and maturation. Biochim Biophys Acta (BBA) Mol Cell Res 1853:1350–69. https://doi.org/10.1016/j.bbamcr.2014.11.021

Pinske C, Sawers RG (2016) Anaerobic formate and hydrogen metabolism. Eco Sal Plus, ESP-0011-2016. https://doi.org/10.1128/ecosalplus.ESP-0011-2016

Piskarev IM, Ushkanov VA, Aristova NA, Likhachevet PP, Myslivets TS (2010) Establishment of the redox potential of water saturated with hydrogen. Biophys J 55:13–17. https://doi.org/10.1134/S0006350910010033

Poladyan A, Avagyan A, Vassilyan A, Trchouninan A (2012) Oxidative and reductive routes of glycerol and glucose fermentation by *Escherichia coli* bath cultures and their regulation by oxidizing and reducing reagents at different pHs. Curr Microbiol 65:N5. https://doi.org/10.1007/s00284-012-0240-2

Poladyan A, Trchounian K, Sawers RG, Trchounian A (2013) Hydrogen-oxidizing hydrogenases 1 and 2 of *Escherichia coli* regulate the onset of hydrogen evolution and ATPase activity,

respectively, during glucose fermentation at alkaline pH. FEMS Microbiol Lett 348:143–148. https://doi.org/10.1111/1574-6968.1228

Poladyan A, Trchounian K, Vasilian A, Trchouian A (2018) Hydrogen production by *Escherichia coli* using brewery waste: optimal pretreatment of waste and role of different hydrogenases. Renew Energy 115:931–936. https://doi.org/10.1016/j.renene.2017.09.022

Poladyan A, Blbulyan S, Sahakyan M, Lenz O, Trchounian A (2019) Growth of the facultative chemolithoautotroph *Ralstonia eutropha* on organic waste materials: growth characteristics, redox regulation and hydrogenase activity. Microb Cell Fact 18:201. https://doi.org/10.1186/s12934-019-1251-5

Poladyan A, Margaryan L, Trchounian K, Trchounian A (2020) Biomass and biohydrogen production during dark fermentation of *Escherichia coli* using office paper waste and cardboard. Intern J of Hyd Energy 45(1):286–293. https://doi.org/10.1016/j.ijhydene.2019.10.246

Poole RK (2016) Preface to Adv in Microb Physiol 580:68. https://doi.org/10.1016/S0065-2911(16)30016-9

Raposo F, Rubia MA, Borja R, Alaiz M (2008) Assessment of a modified and optimised method for determining chemical oxygen demand of solid substrates and solutions with high suspended solid content. Talanta 76(2):448–453. https://doi.org/10.1016/j.talanta.2008.03.030

Roger M, Brown F, Gabrielli W, Sargent F (2018) Efficient hydrogen-dependent carbon dioxide reduction by *Escherichia coli*. Curr Biol 1:140–145. https://doi.org/10.1016/j.cub.2017.11.050

Rossmann R, Sawers G, Böck A. (1991) Mechanism of regulation of the formate-hydrogenlyase pathway by oxygen, nitrate and pH: definition of the formate regulon. Mol Microbiol 5:2807–2814. https://doi.org/10.1111/j.1365-2958.1991.tb01989.x

Seferyan T, Baghdasaryan L, Iskandaryan M, Trchounian K, Poladyan A (2024) Development of an H_2 fuel cell electrochemical system powered by *Escherichia coli* cells. Electrochem Commun 165:1388–2481. https://doi.org/10.1016/j.elecom.2024.107746

Sołowski G, Konkol I, Cenian A (2020) Methane and hydrogen production from cotton waste by dark fermentation under anaerobic and micro-aerobic conditions. Biomass Bioenerg 138:105576. https://doi.org/10.1016/j.biombioe.2020.105576

Spinei M, Oroian M (2021) The potential of grape pomace varieties as a dietary source of pectic substances. References 217(10):867. https://doi.org/10.3390/foods10040867

Taylor MJ, Alabdrabalameer HA, Skoulou V (2019) Choosing physical, physicochemical, and chemical methods of pre-treating lignocellulosic wastes to repurpose into solid fuels. Sustainability 11:3604. https://doi.org/10.3390/su11133604

Trchounian K, Pinske C, Sawers RG, Trchounian A (2012) Characterization of *Escherichia coli* [NiFe]-hydrogenase distribution during fermentative growth at different pHs. Cell Biochem Biophys 62:433–440. https://doi.org/10.1007/s12013-011-9325-y

Trchounian K, Sawers G, Trchounian A (2017) Improving biohydrogen productivity by microbial dark- and photo-fermentations: novel data and future approaches. Renew Sustain Energy Rev 80:1201–1216. https://doi.org/10.1016/j.rser.2017.05.149

Vamvuka D, Elmazaj J, Berkis M (2023) Enhanced H_2 gas production from steam gasification of a winery waste through CO_2 capture by waste concrete fines and use of alkali catalysts. J Renew Energy 219(1):119428. https://doi.org/10.1016/j.renene.2023.119428

Vassilian A, Trchounian A (2009) Environment oxidation-reduction potential andredox sensing by bacteria. In: Trchounian A (ed) Bacterial membranes. Res. Signpost: Kerala (India), pp 163–195

Wang MJ, Wang GZ, Sun ZX, Zhang YK, Xu D (2019) Review of renewable energy-based hydrogen production processes for sustainable energy innovation. Glob Energy Interconnect 2:436–443. https://doi.org/10.1016/j.gloei.2019.11.019

Wood TK, Maeda T, Sanchez-Torres V (2007) Enhanced hydrogen production from glucose by metabolically engineered *Escherichia coli*. Appl Microbiol Biotechnol 77(4):879–890. https://doi.org/10.1007/s00253-007-1217-0

2020 world wine production first estimates, International Organisation of Vine and Wine Intergovernmental Organisation 2020. https://www.oiv.int/2020-world-wine-production-first-estimates

Xue YS, Jian PT, Ning H, Swee KY, Yew WH, Abdullah AIL, Shareena FAlM, Nurul AB, Jamali NS (2023) Unraveling the effect of redox potential on dark fermentative hydrogen production. Renew Sustain Energy Rev 187:113755. https://doi.org/10.1016/j.rser.2023.113755

Zavala-Méndez M, Vargas A, Carrillo-Reyes J (2022) Maximization of bio-hydrogen production from winery vinasses using on-line feedback control. Int J Hyd Energy 78:33259–33271. https://doi.org/10.1016/j.ijhydene.2022.07.196

Zhang L, Ong J, Liu J, Fong Yau Li S (2017) Enzymatic electrosynthesis of formate from CO_2 reduction in a hybrid biofuel cell system. J Renew Energy 108:581–588. https://doi.org/10.1016/j.renene.2017.03.009

Zhang L, Zhang J, Loh KC (2019) Enhanced biogas production from anaerobic digestion of solid organic wastes: current status and prospects. Bioresour Technol Rep 5:280–296. https://doi.org/10.1016/j.biteb.2018.07.005

Zhao J, Patwary AK, Qayyum A, Alharthi M, Bashir F, Mohsin M, Hanif I, Abbas Q (2022) The determinants of renewable energy sources for the fueling of a green and sustainable economy. J Energy 238:122029. https://doi.org/10.1016/j.energy.2021.122029